Development of a hydraulic system for the mitigation of end-effector collisions

G. Cipriani, D. Tommasino, M. Bottin, A. Doria and G. Rosati

Abstract The increasing number of artificial intelligence (AI) applications, and the adoption of collaborative robots in the industry are rising the necessity for the development of systems and algorithms able to detect and mitigate collisions. These are due to the probabilistic nature of AI applications and the environment. Indeed, an AI can perform poorly in unpredictable scenarios, and a cobot may face a distracted operator. These scenarios result in an unsafe situation where the robot impacts with its external environment. Solutions must be developed to mitigate these impacts with obstacles and manipulated objects. This paper presents a hydraulic module to be interposed between the end-effector and the robot flange. This module decouples the end-effector from the robot along the approach axis of the end-effector, thus mitigating the effects of accidental collisions occurring in such direction. Numerical results show the pros and cons of the new system.

1 Introduction

The development of autonomous and collaborative applications in industrial robotics led to the necessity for an additional level of safety standards [1, 2]. For example, some artificial intelligence algorithms can learn a task without proper teaching from an operator. Algorithms such as Reinforcement Learning (RL) learn through a trial and error approach. They try to maximize a reward function. This approach forces the training to be executed in a simulated environment to reduce the possible damages caused by the trial and error approach [3]. However, since the accuracy achieved in simulation depends on the model quality and precision, the accuracy shown in real environments is lower than in the simulated one and collisions with obstacles and manipulated objects are possible. Other risky examples are related to collaborative applications or to teleoperation tasks with an inexperienced operator where the presence of a human operator adds even more unpredictability.

University of Padova, Padua, Italy, e-mail: giulio.cipriani@phd.unipd.it

This work follows the one described in [4], and it is related to the handling of small objects with a mass lower than 1 kg. The previous work exploits a mechanical system composed of a bistable mechanism to mitigate the collisions between the robot and objects disposed on a plane. Mechanical systems guarantee an instantaneous response to the impact delaying the effective impact between the robot and the object. In this way, the robot has the time to adapt to the impact. Moreover, the bistable mechanism passively reduces the momentum transferred to the objects, limiting their movement range after the impact.

This mechanical mitigation system is necessary because the impacts with small objects cannot deform the robot or disturb its motion [5, 4]. Consequently, the robot does not dampen the collision, and the objects are shoot away.

In this paper, the bistable mechanism is replaced with a hydraulic system constituted of a hydraulic cylinder that communicates with an external tank and a gas chamber. The hydraulic system and its mathematical model are described in detail in Section 2. In Section 3, simulated results are presented, and the hydraulic system is compared with the bistable mechanism. Conclusions are drawn in Section 4.

2 Hydraulic compliant system

The hydraulic system is installed between the robot flange and the end-effector and consists in a main hydraulic cylinder connected to an external auxiliary cylinder, by means of an orifice. The auxiliary cylinder is divided in two chambers by a floating piston. The first chamber is filled by the liquid that has moved from the main to the auxiliary cylinder. The second chamber is filled with gas pressurized by a pneumatic line. Figure 1 schematizes the hydraulic system.

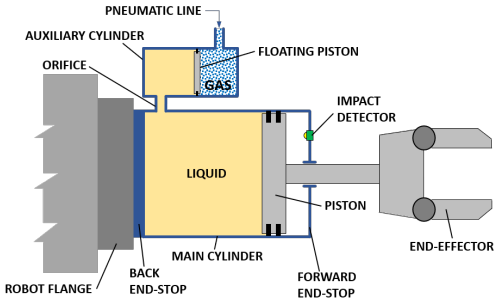

Fig. 1: Scheme of the end-effector with the hydraulic compliant system.

The end-effector moves backwards when a collision with an object occurs, since the dynamics of the end-effector and the robot are decoupled. After the collision, the liquid is forced to flow from the main cylinder to the auxiliary cylinder, through the

orifice. The pressure drop through the orifice and the increase in pressure due to gas compression gradually reduce the relative velocity between the end-effector and the robot, avoiding hard impacts. Indeed, the movement of the end-effector is restricted by the robot flange on one side and by a mechanical end-stop on the other side.

The compliant system is equipped with an impact detector based on a magnetic sensor. This sensor switches on when the piston moves away of 1.5 *mm* from the forward end-stop. Therefore, the robot can detect the collision and react, for instance by stopping its movement. It is worth noticing that the robot is characterized by a delay in the reaction to the collision, due to the time needed to the detection and the processing of the signal from the impact detector (*dead time*) [6, 7]. The *dead time* is a feature of the considered robot and signal processing system.

The hydraulic system is designed to adapt its compliance to different scenarios. By adjusting the pressure of the gas, the robot can perform specific tasks, such as assembling or plugging, for which a completely compliant system would be not suitable. In addition, the gas in the auxiliary cylinder is pressurized to pre-load the end-effector, preventing movements due to robot accelerations, and to restore the initial position of the end-effector after the collision.

The presented design can be extended to a compliant system acting in multiple directions. Relying on [2] in which the mathematical model of a N-DOF compliant structure is presented, a set of hydraulic systems arranged in series and connected by pre-loaded hinges is able to absorb unexpected collisions from multiple directions.

2.1 Mathematical model

The mathematical model analyses the collision between a small object (hundreds of grams) and the end-effector with the hydraulic compliant system. The simulations aim to highlight the effects of this decoupling system in terms of mitigation of collisions on the robot, the end-effector and the object. The analysis considers only a one-dimensional model of the collision, since it is assumed that the end-effector approaches the object along a linear trajectory. The links of the robot are assumed rigid, and the joints are assumed without compliance and clearances, since the stiffness of links and joints are much larger than the stiffness of the decoupling system [8, 5]. Hence, the robot is equivalent to a rigid plate, moving along the direction of approach with a trapezoidal velocity profile. The end-effector and the object are modelled as lumped masses. The hydraulic decoupling system is schematized using a non-linear lumped parameter model. Three phenomena are considered in the lumped model of the hydraulic system [9]:

- The pressure drop through the orifice, having a diameter much smaller than the diameter of the main cylinder, which is given by:

$$\Delta p = \frac{1}{2} c_0 \rho_L \frac{A_p^2}{A_o^2} (\dot{x}_r - \dot{x}_t)^2 \tag{1}$$

where c_0 is a coefficient, ρ_L is the liquid density, A_p and A_o are the areas of the main cylinder and the orifice respectively, $\dot{x}_r$ and $\dot{x}_t$ are the velocities of the robot and the tool respectively.

- An adiabatic variation in gas pressure in the auxiliary cylinder is assumed. Hence, gas pressure p_1 is given by the following equation:

$$p_1(t) = \frac{p_{10} \cdot V_{g,0}^k}{V_g(t)^k} \tag{2}$$

where p_{10} and $V_{g,0}$ are the initial pressure and volume of the gas; k is the adiabatic constant of the gas ($k = 1.4$); V_g is the effective volume of the gas chamber.

- The friction force between the pistons and the cylinders, which includes both a dry friction term (coefficient d) and a viscous term (coefficient b) [9]:

$$F_f = d \cdot \text{sgn}(\dot{x}_r - \dot{x}_t) + b \cdot (\dot{x}_r - \dot{x}_t) \tag{3}$$

Figure 2 shows the lumped parameter model. The variables x_r, x_t and x_p are the coordinate of the robot flange, the end-effector and the object, respectively.

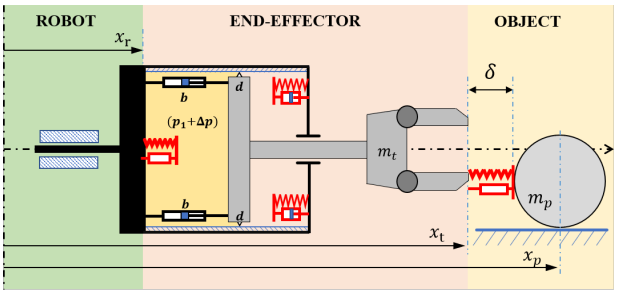

Fig. 2: Lumped parameter model of the system.

The equations of motions of end-effector and object during the collision are:

$$\begin{aligned} m_t \ddot{x}_t &= (p_1 + \Delta p) \cdot A_p - F_c + F_f \\ m_p \ddot{x}_p &= F_c \end{aligned} \tag{4}$$

in which m_t and m_p are the mass of the end-effector and the object, respectively; F_c is the contact force between the end-effector and the object, which is expressed using a non-linear contact model as presented in [4, 10]:

$$F_c = k_c \delta^{3/2} + \chi_c \delta^{3/2} \dot{\delta} \tag{5}$$

where k_c and χ_c are constants.

The force on the robot due to the collision is calculated as follows:

$$F_r = -(p_1 + \Delta p) \cdot A_p - F_f + F_{f,e} + F_{b,e} \tag{6}$$

in which $F_{f,e}$ and $F_{b,e}$ are the contact force due to the impact between the piston of the end-effector and the forward and backward end-stops. These forces are expressed using the same non-linear formulation presented in [6].

The non-linear analytical model was implemented in MATLAB to carry out the simulations presented in the following section.

3 Numerical results and comparison with bistable mechanism

The results of the numerical simulations of the end-effector with the hydraulic system are presented and compared with the ones obtained with the bistable mechanism. It is assumed that the robot approaches the object with a trapezoidal velocity profile and stops, when the collision is detected, after a certain dead time (DT). The simulations were carried out using the values in Table 1. The parameters L, R_p and R_o represent the stroke of the piston, the radius of the main cylinder and the radius of the orifice, respectively. $\dot{x}_{r_{max}}$ is the robot velocity before the impact with the objects.

Table 1: Values of the parameters of the model used in simulations.

Parameter	*Unit*	*Value*	*Parameter*	*Unit*	*Value*
$\mathbf{L}$	m	0.023	$\mathbf{m_t}$	kg	0.048
$\mathbf{R_p}$	m	0.020	$\mathbf{m_p}$	kg	0.246
$\mathbf{R_o}$	m	0.008	$\mathbf{p_{10}}$	Pa	1000
$\mathbf{c_0}$	/	3	$\mathbf{V_{g,0}}$	m^3	$7.63 \cdot 10^{-5}$
$\mathbf{b}$	kgs^{-1}	0.5	$\rho_\mathbf{L}$	kgm^{-3}	900
$\mathbf{d}$	N	0	$\dot{\mathbf{x}}_{r_{max}}$	ms^{-1}	1
$\mathbf{k_c}$	$Nm^{-1.5}$	$0.6 \cdot 10^6$	$\chi_\mathbf{c}$	$Nsm^{1/2}$	$1.35 \cdot 10^6$

Figure 3 shows the calculated positions and velocities. The vertical line represents the time at which the sensor detects the impact. A dead time $DT = 70\ ms$ is assumed.

At the impact, the end-effector is slowed down. Then, after the initial transient, the end-effector and the object move together. Therefore, the object is exerting a force on the end-effector that keeps active the flow between the chambers. The end-effector continues moving backwards until the pressure in the gas chamber stops the flow. In Figure 3c the pressure inside the gas chamber is depicted. It can be observed that the pressure has a maximum in correspondence to the instant in which the robot starts decelerating. The velocity of the end-effector is larger than the velocity of the robot during braking, hence gas expands.

To analyze the performance of the system, Figures 4a and 4b show the position and velocity plots of the bistable mechanism proposed in [4]. Both systems have a non-linear behavior. However, since the bistable mechanism exploits a mechanical phenomenon, its dynamics are more jerky. Consequently, the forces exerted on the robot include large impulses (see Fig. 4b). Moreover, the final velocity of the object

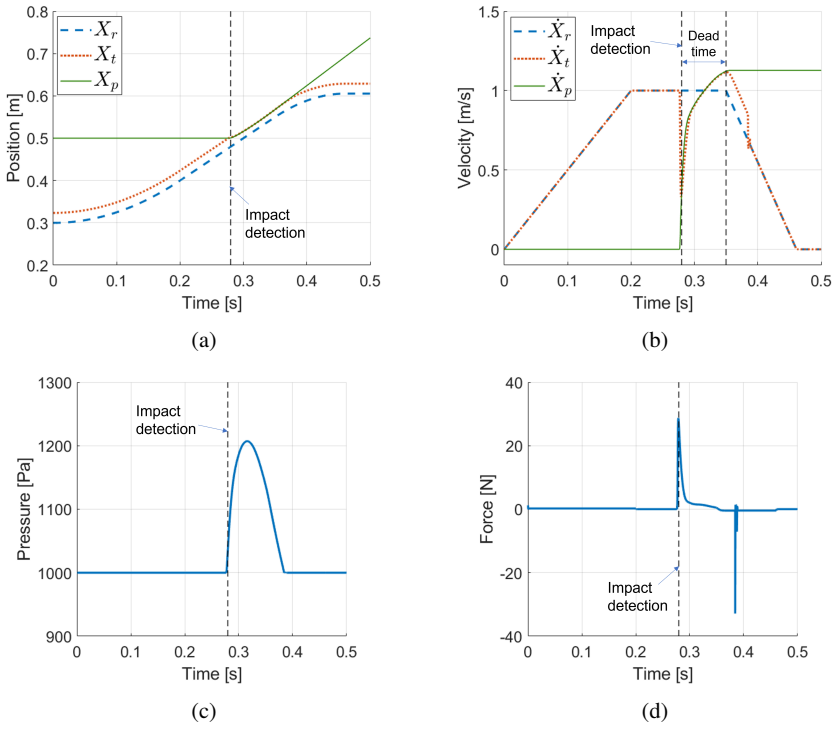

Fig. 3: Simulation results for hydraulic system with $DT = 70\ ms$: (a) positions and (b) velocities for robot $(X_r, \dot{X}_r)$, end-effector $(X_t, \dot{X}_t)$ and object $(X_p, \dot{X}_p)$; (c) pressure inside the gas chamber and (d) force on the robot F_r.

is lower with the hydraulic system than the one reached with the bistable mechanism. This result is true when there is a certain dead time between the detection time and the reaction time. Figures 4 and 5 show that the object velocity with the bistable mechanism depends on the number of collisions with the end-effector. If the dead time is low and the subsequent impacts happen when the robot has already decelerated, the bistable mechanism is more efficient regarding to momentum reduction.

The forces with the hydraulic system are lower than the ones with the bistable mechanism, as can be inferred from Figure 6. It can be seen that the peaks appear on different instants. For the hydraulic system, there are two main peaks. The first corresponds to the impact with the object, whereas the second (having opposite sign) corresponds to the impact of the end-effector with the front end-stop. Since the end-effector is pushed back to the starting position when the gas pressure is released. Conversely, the bistable mechanism shows three peaks. The first corresponds to the impact with the object and its the minor of the three. The second and the third correspond to impacts with the back end-stop. They are caused by the presence of the spring that pushes the end-effector against the back end-stop. In conclusion, with the

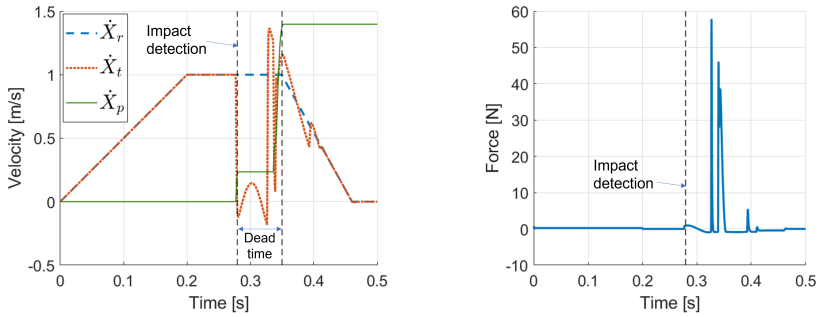

(a) (b)

Fig. 4: Simulation results for bistable mechanism [4] with same general parameters as the hydraulic one. (a) velocities of the three components of the systems; (b) force on the robot F_r.

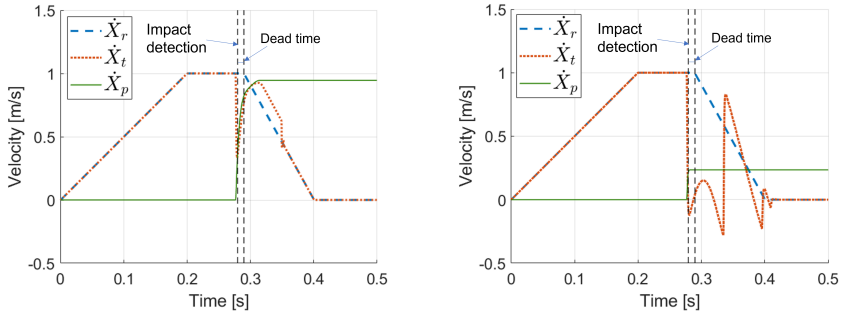

(a) (b)

Fig. 5: Comparison between velocities with $DT = 10\ ms$ of delay after the impact for the (a) hydraulic system and (b) bistable mechanism.

hydraulic system, the maximum force is reached when the end-effector impacts the object, whereas with the bistable mechanism when the end-effector impacts with the back end-stop. This explains why the bistable mechanism transfers less momentum to the object in the first collision.

4 Conclusions

The hydraulic system proposed in this paper is able to mitigate the impacts between the robot and small objects disposed on a plane. Simulations showed that the hydraulic system can outperform the bistable mechanism proposed in a previous

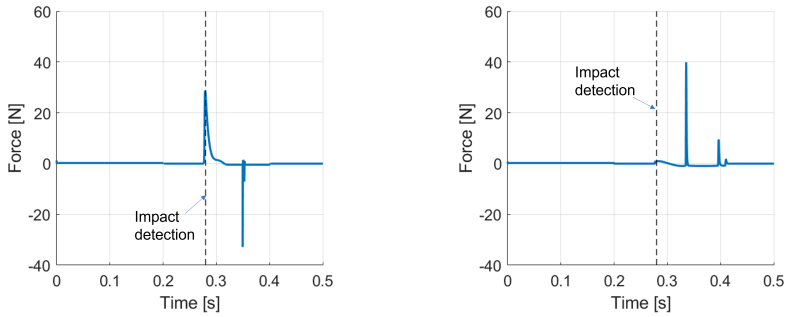

Fig. 6: Comparison between forces exerted on the robot with $DT = 10\ ms$ of delay after the impact for the (a) hydraulic system and (b) bistable mechanism [4].

research, since smaller forces on the robot and a smoother movement of the compliant system are obtained. Another advantage is the easiness of regulation, since the pressure of the gas is the only variable of the system. This is an important property when there is high variability in the environment. However, the bistable mechanism provides a larger reduction in the momentum transferred to objects, when the dead time is small.

References

1. Yuval, C., et al.: Deploying cobots in collaborative systems: major considerations and productivity analysis. Int. J. of Production Research **0**(0), 1–17 (2021)
2. Seriani, S., et al.: Development of n-DoF Preloaded Structures for Impact Mitigation in Cobots. J. of Mechanisms and Robotics **10**(5) (2018)
3. Lobbezoo, A., et al.: Reinforcement learning for pick and place operations in robotics: A survey. Robotics **10**(3) (2021)
4. Tommasino, D., et al.: Effect of end-effector compliance on collisions in robotic teleoperation. Applied Sciences **10**(24) (2020)
5. Doria, A., et al.: Analysis of the compliance properties of an industrial robot with the mozzi axis approach. Robotics **8**(3) (2019)
6. Tommasino, D., et al.: Development and Validation of an End-Effector for Mitigation of Collisions. J. of Mechanical Design **144**(4) (2021)
7. Tommasino, D., et al.: Development of an end-effector for mitigation of collisions. Volume 7: 17th IEEE/ASME Int. Conf. Mechatron. Embed. Syst. Appl. MESA (2021)
8. Bottin, M., et al.: Modeling and identification of an industrial robot with a selective modal approach. Applied Sciences **10**(13) (2020)
9. Cossalter, V., et al.: On the non-linear behaviour of motorcycle shock absorbers. Proc. of the Institution of Mech. Eng., Part D: J. of Automobile Engineering **224**(1), 15–27 (2010)
10. Skrinjar, L., et al.: A review of continuous contact-force models in multibody dynamics. International Journal of Mechanical Sciences **145**, 171–187 (2018)